Designing Aligned Inorganic Nanotubes at the Electrode Interface: Towards Highly Efficient Photovoltaic Wires

*Tao Chen, Longbin Qiu, Hamid G. Kia, Zhibin Yang, and Huisheng Peng**

Due to the large surface area and remarkable electronic property, carbon nanotubes (CNTs) have been widely explored to fabricate organic photovoltaics with a high efficiency.[1–3] They can be either directly incorporated into active layers to improve charge separation and transport, or coated into films to replace conventional electrode materials such as indium tin oxide or platinum (Pt) in the case of a dye-sensitized solar cell.[4–9] However, CNTs are randomly aggregated in the active layer or electrode film by a typical solution process, which has largely limited their performance, e.g., the produced electrons have to cross a lot of boundaries in random CNT networks.[10–12] Therefore, increasing attentions are recently paid to preparing highly aligned CNT materials, mainly in a film format for electrodes of organic solar cells and organic light-emitting diodes.[13–16] For instance, dye-sensitized solar cells could be fabricated by using an aligned CNT sheet as counter electrode to replace Pt due to the combined high electrocatalytic and electrical properties.[15,16] The energy conversion efficiency of the resulting cell was much higher than the randomly dispersed CNT film and comparable with Pt.[16] Similarly, in the case of dye-sensitized solar cells, a layer of three-dimensional network composed of titanium dioxide (TiO_2) nanoparticles was generally used as a supporting material of dyes and transporting medium of electrons in working electrodes.[17] However, the transport efficiency of electrons was also hindered by the high number of boundaries among TiO_2 nanoparticles, which decreased their electron mobility with a low energy conversion efficiency.[18,19] Therefore, aligned TiO_2 nanotubes has been proposed and studied to greatly enhance light harvesting, electron collection, and ion diffusion at the TiO_2–electrolyte interface.[14,20]

Although it had been widely explored to increase the energy conversion efficiency of above planar photovoltaic device by introducing and optimizing the nanostructure of electrode interface,[14–16] it is rare for wire-shaped photovoltaic devices which can be easily woven into lightweight textiles with unique advantages.[21–23] Recently, CNTs and TiO_2 nanomaterials had been successfully used as electrodes for a wire-shaped dye-sensitized solar cell.[7] Here TiO_2 nanotubes were highly aligned on the titanium wire as the working electrode, and the CNTs were then coated on the outer surface as a counter electrode by a solution process. However, as the CNTs were randomly dispersed to form a network structure which was unfavorable for the rapid charge separation and transport,[10–12] a low energy conversion efficiency of 1.6% was observed for a freestanding wire cell, and it would be also difficult to improve the cell efficiency.[7] In addition, for a thin CNT film with thickness of 20–40 nm, it remains challenging to produce a uniform structure, and the cell performance may be not stable and repeatable.

Herein, we have developed a new structure of dye-sensitized photovoltaic wires (**Figure 1**). An aligned CNT fiber with good structure control, high electrocatalytic activity, high mechanical strength, and unique three-dimensional hopping conduction[2] is used as a counter electrode, while a titanium wire with perpendicularly aligned titanium dioxide nanotubes grown on the outer surface is used as the working electrode. The two electrodes are twined to produce the desired photovoltaic wire. Dye molecules are chemisorbed on TiO_2 nanotubes to generate electrons upon absorption of light. The generated electrons are injected into the conduction band of TiO_2 nanotubes and transported along the titanium wire. The electrons reach the CNT fiber through the external circuit. Dye cations are reduced to the ground state by oxidation of I^- into I_3^- ions, while I_3^- is reduced to I^- by accepting electrons at the CNT fiber. Due to the high surface area and aligned structure of both CNTs and TiO_2 nanotubes, the charge can be rapidly separated and transported, so the resulting wire cell showed a high performance, e.g., an energy conversion efficiency up to ~4.6%.

CNT fibers could be spun from a CNT array at a large scale (see Figure S1).[2] The diameter of CNT fibers was in the range of 10 to 30 μm, and the used CNTs showed a double-walled structure with diameter of ~6.5 nm. **Figures 2**a and 2b show scanning electron microscopy (SEM) images of aligned CNTs in a fiber. The CNT fiber has a low density of 0.8 g cm^{-3}, a high tensile strength of ~ 600 MPa (Figure S2), and an excellent electrical conductivity of 10^3 S cm^{-1}. Different from a random CNT network in which electrons have to cross a lot of boundaries during the transport, they can be more effectively transported along the axial direction of aligned CNTs based on a three-dimensional conduction model of CNT fiber.[2]

Growth of aligned TiO_2 nanotubes in the radial direction of titanium wire was made by electrochemically anodizing a pure titanium wire (Figure S3). Figures 2c and 2d show representative SEM images of aligned TiO_2 nanotubes on the outer surface of a titanium wire. Figures 2d and 2e further show that the diameters of TiO_2 nanotubes are ranged from 70 to 100 nm with a wall thickness of 25 nm from top and side views, respectively. We had also peeled off the TiO_2 nanotubes and investigated

T. Chen, L. Qiu, Z. Yang, Prof. H. Peng
State Key Laboratory of Molecular Engineering of Polymers
Department of Macromolecular Science and Laboratory of Advanced Materials
Fudan University
Shanghai 200438, China
E-mail: penghs@fudan.edu.cn.
Dr. H. G. Kia
Chemical Sciences and Materials Systems Lab
GM Global R&D, 30500 Mound Road, Warren, MI 48090, USA.

DOI: 10.1002/adma.201201893

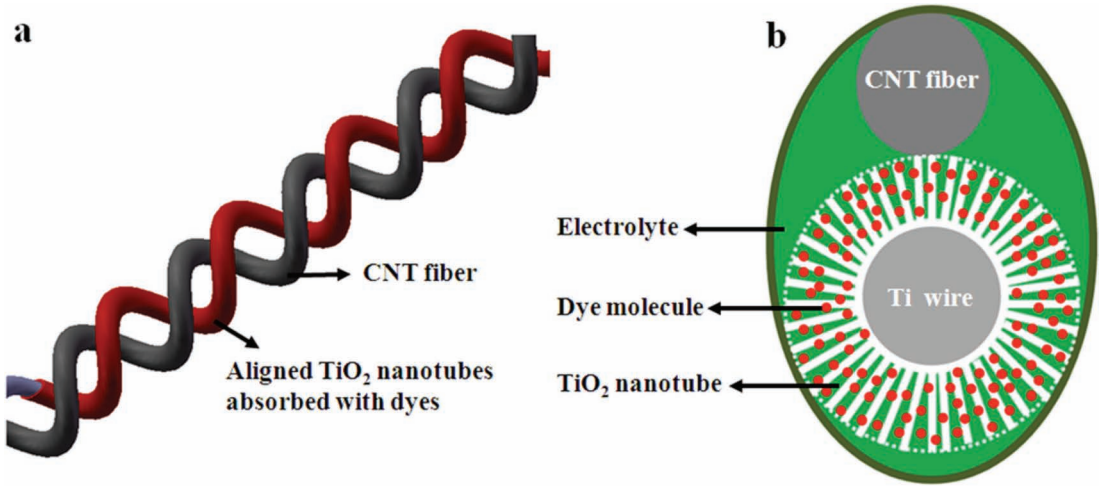

Figure 1. Schematic illustration to the wire-shaped dye-sensitized solar cell by (**a**) side and (**b**) top views. Here an aligned TiO_2 nanotube-modified titanium wire as the working electrode is twined with an aligned CNT fiber as the counter electrode to produce the wire cell.

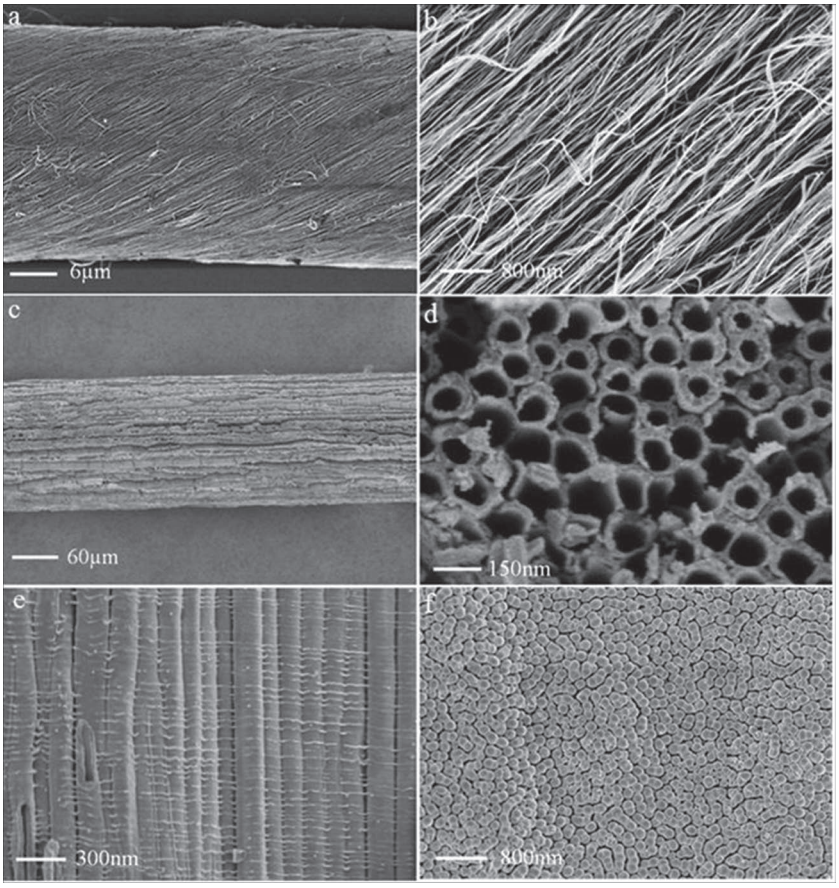

Figure 2. Scanning electron microscopy (SEM) images of CNT fiber and TiO_2 nanotube-modified titanium wire being anodized at the voltage of 60 V, reaction time of 2 h, and water concentration of 1%. (a) A CNT fiber at low magnification. (b) A CNT fiber at high magnification. (c) A titanium wire grown with aligned TiO_2 nanotubes perpendicular to its outer surface. (d) Top view of aligned TiO_2 nanotubes. (e) Side view of aligned TiO_2 nanotubes. (f) Bottom view of aligned TiO_2 nanotubes after removal from the titanium wire.

their bottom ends in Figure 2f. Obviously, the resulting TiO_2 nanotubes are uniform in diameter. The length of TiO_2 nanotubes was easily tuned by varying the anodizing time. For instance, their lengths were increased from 11 to 15, 22, 35, and 40 μm with the increase in anodizing time from 2 to 4, 6, 8, and 10 h, respectively. The nanostructures of TiO_2 nanotubes were mainly controlled by varying the voltage from 40 to 80 V and water concentration from 0.5 to 2% in the electrolyte. Highly aligned and intact TiO_2 nanotubes were mainly obtained at the anodizing voltage of 60 V (Figure S4). A higher or lower voltage produced non-uniform or branched structure. Similarly, aligned and uniform TiO_2 nanotubes were grown at a water concentration of 1% (Figure S5). Very short and randomly aggregated TiO_2 nanotubes had been observed at lower water concentrations, while broken or defected TiO_2 nanotubes had been synthesized at higher water concentrations. Note that a ripple-like structure was observed on the outer surface of TiO_2 nanotubes. This structure may be ascribed to the current or voltage oscillation which was believed to be resulted from the variation of electrolyte concentration during the anodization process,[24] though the mechanism is yet to be verified.

The fabrication of photovoltaic wire is described in the Experimental Section. To summarize, a CNT fiber and a TiO_2 nanotube-modified titanium wire absorbed with the dye of [*cis*-bis(isothiocyanato)bis(2,2′-bipyridyl-4,4′- dicarboxylato) ruthenium(II)

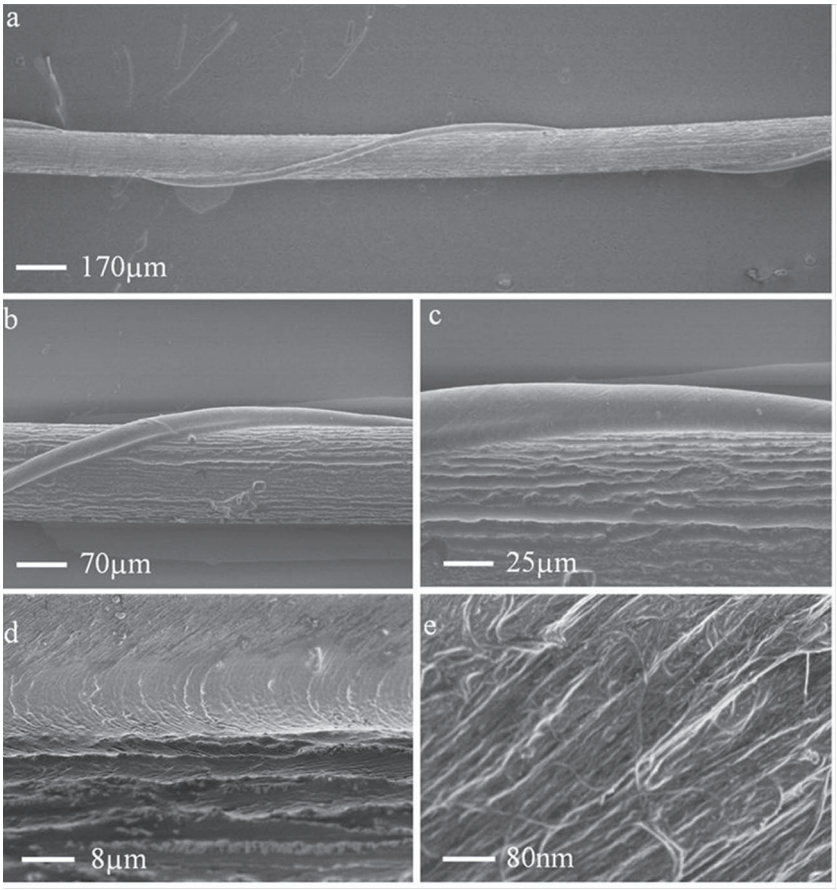

Figure 3. SEM images of a photovoltaic wire by using the CNT fiber as a counter electrode and TiO_2 nanotube-modified titanium wire as the working electrode. (a) Low magnification. (b) and (c) High magnification of a twined part. (d) A typical contacting interface between the two electrodes. (e) High magnification of the CNT fiber in the cell.

bistetrabutylammonium] (N719, chemical structure shown in Figure S6) were twined with different thread pitches. Photographs of a cell fabrication are shown in Figure S7. Both CNT fiber and TiO_2 nanotube-modified titanium wire were fixed on a glass slide using indium through an ultrasonic welding technique. **Figure 3**a shows part of a photovoltaic wire with a screw pitch of 1.8 mm. Under higher magnifications in Figures 3b–3d, the two electrodes are closely contacted for effective charge separation and transport. In addition, the CNTs remained highly aligned in structure when the wire device was bent for many cycles, which is critical for the redox reaction of I^-/I_3^- and electron transport (Figure 3e).

The plot of current density versus voltage (J–V curve) shows the open-circuit voltage (V_{oc}), short-circuit current density (J_{sc}) and fill factor (FF), from which power conversion efficiency (η) is calculated according the equation of $\eta = FF \times V_{oc} \times J_{sc}/P_{in}$, where P_{in} is the incident light power density. The cell performance depended on the diameter of the CNT fiber. As shown in Figure S4, the efficiency increases with the increasing diameter because more CNTs provide more active sites in catalyzing the redox reaction of I^-/I_3^-. Both structure and size of TiO_2 nanotubes also affected the performance of photovoltaic wires. TiO_2 nanotubes which were synthesized under different experimental conditions had been carefully compared under a standard illumination (AM 1.5, 100 mW cm^{-2}). Different voltages were first investigated while the other experimental parameters were kept the same. It was found that the anodization at 60 V provided the wire cell with the highest energy conversion efficiency of 2.04% (**Figure 4**a). The lower or higher voltages decreased the efficiency of the cell, e.g., 1.60% at 40V and 0.73% at 80V. The concentration of H_2O in the electrolyte also played a critical role on the cell efficiency. Figure 4b compares J–V curves of wire cells with TiO_2 nanotubes being synthesized in the electrolyte containing increasing water concentrations from 0.5 to 2% with the same anodizing voltage of 60V and time of 2 h. The optimal H_2O concentration occurred at 1%. The different efficiencies were mainly ascribed to the structural order and the integrity of TiO_2 nanotubes.[25] For instance, high-quality TiO_2 nanotubes were aligned and closely attached on the titanium wire at an anodizing voltage of 60 V while they easily broke and were peeled off the core titanium wire at an anodizing voltage of 80 V (Figures S5 and S8).

The length of TiO_2 nanotubes also plays a critical role in the photovoltaic performance as it determines the quantity of loaded dye molecules and the transport distance of electrons from the TiO_2 nanotubes to the Ti wire. More dye molecules will be loaded on the TiO_2 nanotubes with the increasing length of TiO_2 nanotubes, which improves the cell efficiency. However, longer TiO_2 nanotubes will also increase the transport distance of electrons, which causes more undesirable charge recombination with a lower cell efficiency. An optimal length should exists for the dye-sensitized solar cell based on TiO_2 nanotubes. Here the length of TiO_2 nanotube can be controlled from 10 to 40 μm (Figure S9) by increasing the anodizing time from 2 to 10 h. The short-circuit current density increased from 5.78 to 9.84 mA cm^{-2} with the increase of anodizing time from 2 to 8 h, and then decreased to 8.04 mA cm^{-2} with the further increase to 10 h, while both V_{oc} and FF remain almost unchanged (Figure 4c). The representative J–V curves are shown in Figures S10–S14, and the photovoltaic parameters are further summarized in Tables S1–S5 in the Supporting Information. Obviously, the highest energy conversion efficiency (3.9%) can be obtained when the length of TiO_2 nanotube was ~35 μm at the anodizing time of 8h.

The pitch distance is expected to obviously affect the energy conversion efficiency of the wire cell. A lower screw pitch increases the contact point with a higher charge transport efficiency, which can improve the short-circuit current density. Figure 4d compares three photovoltaic wires with different screw pitches. The short-circuit current density at a screw pitch of 0.8 mm is obviously higher than that at a screw pitch of 1.4 mm, while the open-circuit voltage and fill

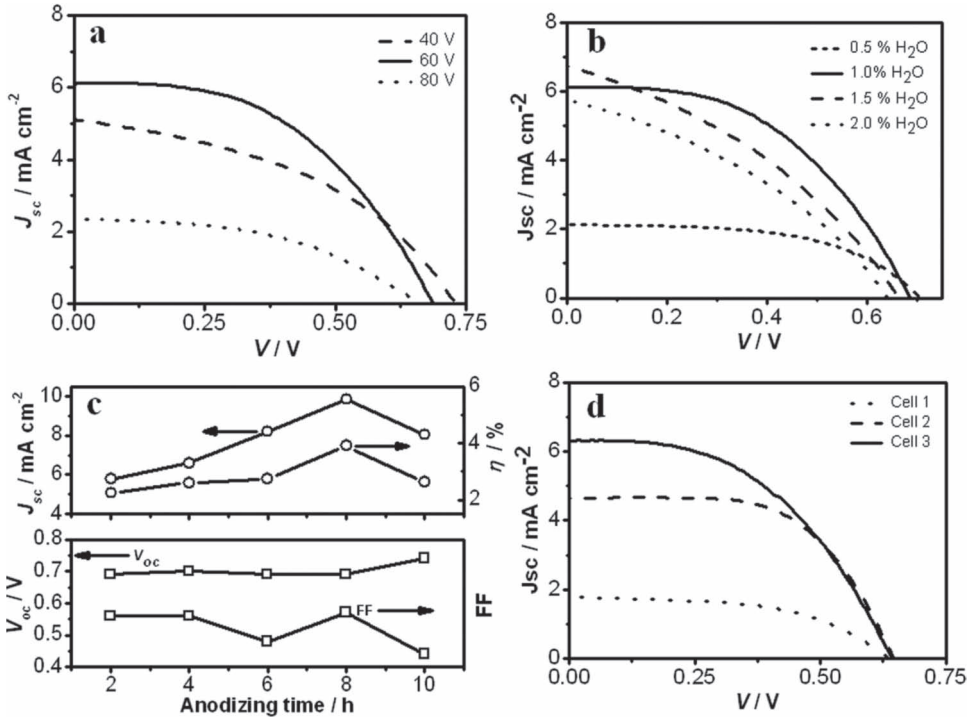

Figure 4. Photovoltaic performance of solar power wires. (a) *J–V* curves by using TiO_2 nanotube-modified titanium wire being anodized at different voltages in the electrolyte containing 1% of H_2O for 2h. (b) *J–V* curves by using TiO_2 nanotube-modified titanium wire being anodized in the electrolyte with different concentrations of H_2O at 60V for 2h. (c) Dependence of J_{sc}, V_{oc}, FF, and η on the anodizing time in the electrolyte containing 1% of H_2O at 60V. (d) *J–V* curves of the cells with two electrodes being parallel for Cell #1, pitch distance of 1.4 mm for Cell #2, and pitch distance of 0.8 mm for Cell #3. The Ti wire was anodized at 60 V for 2h in the electrolyte containing 1% H_2O.

factor are almost the same. When the two electrodes were parallel in the wire device, the lowest efficiency was observed due to a relatively loose contact. Therefore, the cell efficiency increases with the decrease in screw pitch in the investigated range.

To confirm the high performance of CNT fiber, we had compared the photovoltaic wires by using CNT fiber (diameter of 28 μm) and Pt wire (diameter of 25 μm) as counter electrodes, respectively. The same TiO_2 nanotube-modified titanium wire was used as the working electrode, and the two devices were fabricated under the same condition with a pitch distance of 0.8 mm and Ti wire after anodized for 8 h. The short-circuit current density in the case of CNT fiber was 9.7 mA cm^{-2}, compared with 5.7 mA cm^{-2} for the Pt wire (**Figure 5**a). It was observed that the efficiency of the cell derived from the CNT fiber (2.9 – 3.9%) was much higher than the Pt wire (1.0 – 1.6%). To understand the increased efficiency in the CNT fiber based cell, cyclic voltammetry was performed to compare the redox catalytic properties toward I^-/I_3^- between CNT fiber and Pt wire through a three-electrode system under the same condition (Figure S15). Two redox peaks were clearly observed with the left and right ones corresponding to redox reactions of $3I^- \leftrightarrow I_3^- + 2e$ and $2I_3^- \leftrightarrow 3I_2 + 2e$, respectively. Obviously, both of the two redox peaks in the CNT fiber are larger than the Pt wire, which indicates a better catalytic capability of CNT fiber for the redox reaction of I^-/I_3^- than the Pt wire. We had also compared the photovoltaic wire with the increasing length of 0.2 to 1.4 cm. The photovoltaic parameters had not been obviously changed when the cell length was varied in 0.2 – 1.4 cm, and the power conversion efficiency was almost the same (Figure 5b). In other words, these photovoltaic wires are independent of their lengths, which is critically important for the practical application at large scale.

We had also tried to modify the CNT fiber based cell to further improve the performance. To minimize the light reflection for a higher cell performance, a black substrate was placed under the photovoltaic wire. As shown in Figure 5c, the *J–V* curves are almost the same and the photovoltaic parameters remain unchanged. However, the energy conversion efficiency had been obviously increased if a mirror was placed under the wire cell to utilize the area which was generally not irradiated without the mirror. The highest power conversion efficiency with a mirror achieved 4.6%, compared with 2.87% of a wire cell based on TiO_2 nanotubes as working electrode and Pt as counter electrode,[26] 3.3% based on ZnO nanowires as working electrode and Pt as counter electrode,[23] and 1.6% by using CNT film as counter electrode and 2.6% with further assistance of a second metal wire.[7] In addition, the photovoltaic wires could be easily organized in series and/or parallel connection to control the voltage and/or current output. Figure 5d compares the *I–V* curves of two individual wire devices with V_{oc} of 0.72 V and I_{sc} of 0.12 mA for one and V_{oc} of 0.74 V and I_{sc} of 0.13 mA for the other. In a series connection, the produced V_{oc} of 1.44 V is the sum of V_{oc} of the two individual devices. In a

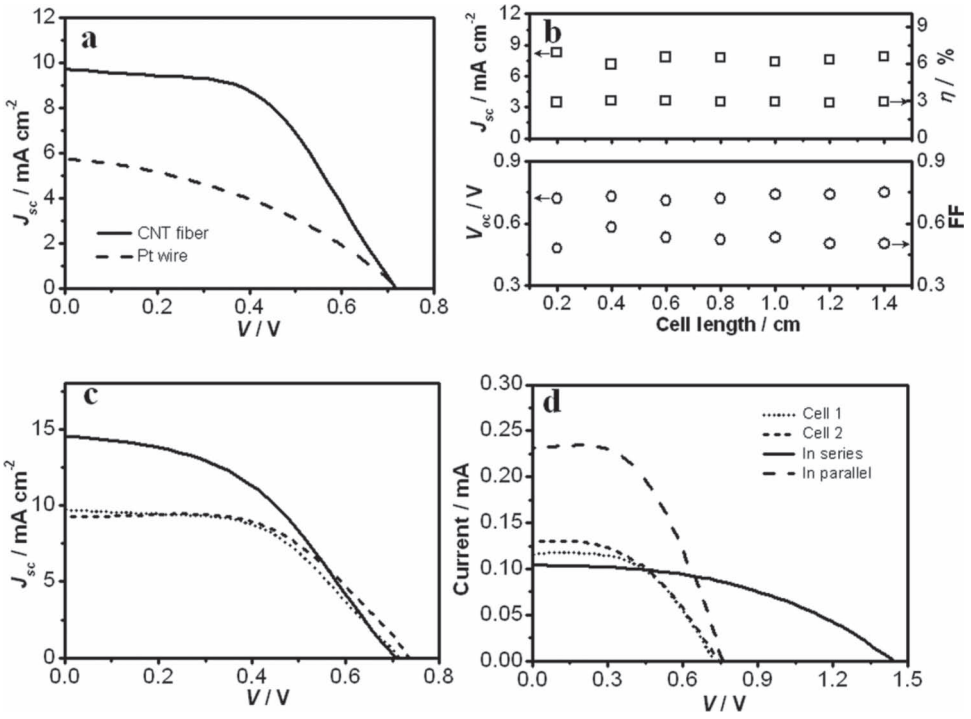

Figure 5. (a) *J–V* curves of dye-sensitized photovoltaic wires based on CNT fiber (solid line) and Pt wire (dash line) as counter electrodes. (b) Dependence of J_{sc}, η, V_{oc} and FF on the cell length. The same Ti wire anodized for 8 h in the electrolyte containing 1% of H_2O at 60V was used. (c) *J–V* curves of a CNT fiber based photovoltaic wire measured at normal condition (dash line), with a mirror under the cell (solid), and with a black substrate under the cell (dot line). (d) *I–V* curves of two individual photovoltaic wires in serial and parallel connections.

parallel connection, the total I_{sc} of 0.23 mA is also equal to the sum of I_{sc} of the two individual devices.

In conclusion, we have studied the performance of dye-sensitized solar power wires by using an aligned CNT fiber as the counter electrode and a titanium wire modified with perpendicularly aligned TiO_2 nanotubes as the working electrode. This novel interface design provides the photovoltaic wire with a high efficiency of 4.6%. The photovoltaic wires can be easily integrated into various flexible devices by a convenient weaving technology, which remain challenging to conventional planar solar cells.

Experimental Section

CNT arrays were synthesized by a chemical vapor deposition in a quartz tube furnace.[2,12] Fe (1.2 nm)/Al_2O_3 (5 nm) on silicon wafer was used as the catalyst, ethylene was used as carbon source with a flowing rate of 90 sccm, a mixture of Ar (480 sccm) and H_2 (30 sccm) was used as carrier gas. The growth was made at 750 °C, and the thickness of spinnable CNT array was about 240 μm. CNT fibers were then spun from the array by using a microprobe with a rotary speed of 2000 rounds per minute.

Highly aligned TiO_2 nanotubes were grown on the titanium wire by electrochemical anodization in 0.25 wt% NH_4F/ethylene glycol solution containing 0.5 to 2 vol% H_2O at different voltages of 40, 60, and 80 V and different residence times of 2 to 10 h. The growth was realized in a two-electrode electrochemical cell with titanium wire (diameter of 127 μm and purity of 99.9%) and Pt wire as anode and cathode, respectively. The resulting wires were washed with deionized water to remove the electrolyte, followed by annealing at 500 °C in air for 1h to produce the anatase TiO_2. The annealed wires were immersed in 0.04 M $TiCl_4$ solution at 70 °C for 30 min, and then rinsed with de-ionized water, followed by annealing again at 450 °C for 30 min. After being cooled to 120 °C, the TiO_2 nanotube-modified titanium wires were immersed into a 0.3 mM N719 solution in alcohol and tert-butyl alcohol with a volume ratio of 1/1. Finally, the dye-absorbed working electrode was twined with a CNT fiber. Prior to characterization, the electrolyte containing 0.1 M LiI, 0.05 M I_2, 0.6 M dimethyl-3-n-propyl-imidazolium iodide, and 0.5 M 4-tert butyl-pyridine in dehydrated acetonitrile was filled into the assembled cell. The wire solar cell can also be packaged into a flexible plastic capillary to meet various applications. The cell was measured by recording *I-V* curves with a Keithley 2400 Source Meter under illumination (100 mW/cm^2) of simulated AM 1.5 solar light coming from a solar simulator (Oriel-Sol3A 94023A equipped with a 450 W Xe lamp and an AM1.5 filter). The light intensity was calibrated using a reference Si solar cell (Oriel-91150). The used area in the calculation of power conversion efficiency was calculated by multiplying the length and diameter of photovoltaic wire.

The structures were characterized by SEM (Hitachi FE-SEM S–4800 operated at 1 kV) and TEM (JEOL JEM–2100F operated at 200 kV). Stress-strain curves were obtained from a Shimadzu Table-Top Universal Testing Instrument. A CNT fiber was mounted on a paper tab with gauge length of 5 mm, and the wire diameter was measured by SEM. The CV study was performed in a three-electrode system on CHI 660a electrochemical workstation at room temperature. An acetonitrile solution containing 0.1 M $LiClO_4$, 5 mM LiI, and 0.5 mM I_2 was used as the electrolyte with Pt wire and Ag/AgCl as counter and reference electrodes, respectively.

Supporting Information

Supporting Information is available from the Wiley Online Library or from the author.

Acknowledgements

This work was supported by NSFC (20904006, 91027025), MOST (2011CB932503, 2011DFA51330), MOE (NCET-09-0318), STCSM (1052nm01600, 11520701400), and General Motors Company. The authors thank Prof. Z.S. Wang for the kind help.

Received: May 10, 2012
Published online: June 21, 2012

[1] L. Hu, D. S. Hecht, G. Grüner, *Chem. Rev.* **2010**, *110*, 5790–5844.
[2] a) T. Chen, S. Wang, Z. Yang, Q. Feng, X. Sun, L. Li, Z. Wang, H. Peng, *Angew. Chem. Int. Ed.* **2011**, *50*, 1815–1819; b) T. Chen, L. Qiu, Z. Cai, F. Gong, Z. Yang, Z. Wang, H. Peng, *Nano Lett.* **2012**, *12*, 2568–2572.
[3] G. Li, F. Wang, Q. Jiang, X. Gao, P. Shen, *Angew. Chem. Int. Ed.* **2010**, *49*, 3653–3656.
[4] S. Berson, R. de Bettignies, S. Bailly, S. Guillerez, B. Jousselme, *Adv. Funct. Mater.* **2007**, *17*, 3363–3370.
[5] C. Li, Y. Chen, Y. Wang, Z. Iqbal, M. Chhowalla, S. Mitra, *J. Mater. Chem.* **2007**, *17*, 2406–2411.
[6] M. W. Rowell, M. A. Topinka, M. D. McGehee, H. J. Prall, G. Dennler, N. S. Sariciftci, L. B. Hu, G. Gruner, *Appl. Phys. Lett.* **2006**, *88*, 233506.
[7] S. Zhang, C. Ji, Z. Bian, R. Liu, X. Xia, D. Yun, L. Zhang, C. Huang, A. Cao, *Nano Lett.* **2011**, *11*, 3383–3387.
[8] W. J. Lee, E. Ramasamy, D. Y. Lee, J. S. Song, *ACS Appl. Mater. Interfaces* **2009**, *1*, 1145–1649.
[9] J. Han, H. Kim, D. Y. Kim, S. M. Jo, S. Jang, *ACS Nano* **2010**, *4*, 3503–3509.
[10] B. Pradhan, S. K. Batabyal, A. J. Pal, *Appl. Phys. Lett.* **2006**, *88*, 093106.
[11] Y. Kanai, J. C. Grossman, *Nano Lett.* **2008**, *8*, 908–912.
[12] H. Peng, *J. Am. Chem. Soc.* **2008**, *130*, 42–43.
[13] K. Jiang, J. Wang, Q. Li, L. Liu, C. Liu, S. Fan, *Adv. Mater.* **2011**, *23*, 1154–1161.
[14] O. K. Varghese, M. Paulose, C. A. Grimes, *Nat. Nanotechnol.* **2009**, *4*, 592–597.
[15] J. E. Trancik, S. C. Barton, J. Hone, *Nano Lett.* **2008**, *8*, 982–987.
[16] a) Z. Yang, T. Chen, R. He, G. Guan, H. Li, L. Qiu, H. Peng, *Adv. Mater.* **2011**, *23*, 5436–5439; b) S. Huang, L. Li, Z. Yang, L. Zhang, H. Saiyin, T. Chen, H. Peng, *Adv. Mater.* **2011**, *23*, 4707–4010.
[17] B. O'Regan, M. Grätzel, *Nature* **1991**, *35*, 737–739.
[18] J. van de Lagemaat, A. J. J. Frank, *J. Phys. Chem. B* **2001**, *105*, 11194–11205.
[19] K. Cassiers, T. Linssen, M. Mathieu, Y. Q. Bai, H. Y. Zhu, P. Cool, E. F. Vansant, *J. Phys. Chem. B* **2004**, *108*, 3713–3721.
[20] K. Zhu, N. R. Neale, A. Miedaner, A. J. Frank, *Nano Lett.* **2007**, *7*, 69–74.
[21] X. Fan, Z. Chu, F. Wang, C. Zhang, L. Chen, Y. Tang, D. Zou, *Adv. Mater.* **2008**, *20*, 592–595.
[22] M. R. Lee, R. D. Eckert, K. Forberich, G. Dennler, C. J. Brabec, R. A. Gaudiana, *Science* **2009**, *324*, 232–235.
[23] B. Weintraub, Y. Wei, Z. L. Wang, *Angew. Chem. Int. Ed.* **2009**, *48*, 8981–8985.
[24] J. H. Yun, Y. H. Ng, C. Ye, A. J. Mozer, G. G. Wallace, R. Amal, *ACS Appl. Mater. Interfaces* **2011**, *3*, 1585–1593.
[25] D. Kim, A. Ghicov, S. P. Albu, P. Schmuki, *J. Am. Chem. Soc.* **2008**, *130*, 16454–16455.
[26] Z. Liu, M. Misra, *ACS Nano* **2010**, *4*, 2196–2200.